Subband gap photoresponse of nanocrystalline silicon in a metal-oxide-semiconductor device

S. M. Hossain,[1,a] A. Anopchenko,[1,b] S. Prezioso,[1] L. Ferraioli,[1] L. Pavesi,[1] G. Pucker,[2] P. Bellutti,[2] S. Binetti,[3] and M. Acciarri[3]

[1]*Laboratorio di Nanoscienze, Dipartimento di Fisica, Università di Trento, Via Sommarive 14, 38100 Povo (Trento), Italy*

[2]*Microtechnologies Laboratory, Fondazione Bruno Kessler, Via Sommarive 18, 38100 Povo (Trento), Italy*

[3]*Dipartimento di Scienza dei Materiali, Università degli Studi Milano-Bicocca, Via Cozzi 53, 20125 Milano, Italy*

(Received 8 July 2008; accepted 22 August 2008; published online 15 October 2008)

In this paper we report on the photoconduction and photovoltaic properties of nanocrystalline silicon. Silicon nanocrystals (Si-ncs) have been prepared by using plasma-enhanced chemical vapor deposition on a *p*-type silicon substrate. The Si-ncs have been formed into the dielectric of a metal-oxide-semiconductor device. *I-V* characteristics of the devices have been studied under dark and illumination. Illumination was performed with light in the wavelength range of 350–1630 nm. A photovoltaic effect has been observed in the illuminated *I-V* characteristics in the range of 350–1100 nm. For longer wavelengths no measurable photovoltaic effect has been observed, but considerable photocurrent has been measured for 1300–1630 nm light under reverse bias condition. This photoresponse is attributed to absorption through subband gap states at the Si-nc and silicon oxynitride matrix interface. © *2008 American Institute of Physics*. [DOI: 10.1063/1.2999561]

I. INTRODUCTION

Metal-oxide-semiconductor (MOS) structures with silicon rich silicon oxide (SRO) containing nanocrystalline silicon have many potential device applications, e.g., high quality memory devices[1–3] and efficient electroluminescent devices.[4–6] Recent studies also show potential in photodetection with high quantum efficiency.[7] Another application field is third generation photovoltaics,[8,9] where the theoretical efficiency of solar cell enriched with silicon nanocrystals (Si-ncs) is well beyond the detailed balance limit of ~31% valid for first generation crystalline silicon solar cells.[10] For silicon solar cells, the efficiency limit is caused by the underutilization of photons with energy higher than the band gap due to thermalization of hot carriers (thermalization losses)[11] and by the nonutilization of subband gap photons present in sunlight (IR losses). On the contrary, in third generation photovoltaics, thermalization losses are reduced by using tandem cells,[12] hot carrier cells,[11] down converter cells,[13,14] and multiple exciton generation (MEG) solar cells.[15–18] IR losses might be overcome by intermediate band solar cells[19] where subband gap photons are absorbed through intermediate level/band present in the band gap (known also as impurity photovoltaic effect[19]) or by coupling the cell with an up-converter material that absorbs two or more subband gap photons and emits photons with energy larger than the band gap of the cell material.[13,20] In all these concepts, nanocrystalline materials are supposed to play an important role.[21,22]

In this work, we have prepared MOS-SRO structures containing nanocrystalline silicon embedded in silicon oxynitride matrix by high temperature annealing of SRO layer grown by plasma-enhanced chemical vapor deposition (PECVD) method. The aim of this work is to assess this material for application in third generation solar cells.

II. EXPERIMENTAL

SRO layers of 50 nm thickness have been deposited on *p*-type (12–18 Ω cm) Si substrate by PECVD technique and annealed at 1050 °C for 1 h to grow Si-nc. A *n*-type polysilicon gate layer (30 nm) has been deposited on the SRO layer. Metallization (a grid) was done by a 500 nm Al (1% Si) thick layer. The gate area was 10.24×10^{-8} m^2. The poly-Si was covered by an antireflective coating formed by a 50 nm thick Si_3N_4 layer and a 120 nm thick SiO_2 layer.

Nitrogen is naturally incorporated in the matrix during the deposition process so that the final dielectric structure is SiO_xN_y. The ratio between the N_2O and the SiH_4 fluxes used during the deposition process was 10. X-ray photoemission spectroscopy analysis gives the following elemental composition (in atomic percent) of the as-deposited SRO layer: 48% of silicon, 47% of oxygen, and 5% of nitrogen. More details on the compositional, optical, and electrical properties of the SRO layer could be found elsewhere.[23]

After annealing, the sample shows a photoluminescence (PL) emission band in the 400–900 nm range under excitation with a 488 nm Ar+ laser. The emission band shows a peak at 790 nm, which in turn corresponds to an optical band gap of 1.6 eV. The average nanocrystal size could be estimated from the emission peak wavelength. Based on some theoretical calculations we estimated the average nanocrystal size of 5 nm.[24] One would conclude a rather different size of nanocrystals, around 3 nm, when using "calibrated" PL results, i.e., the results of reports where the measured PL wavelength was compared with an independently determined

[a]Permanent address: Department of Physics, Bengal Engineering and Science University, Sibpur, India.

[b]Electronic mail: anopchenko@science.unitn.it.

 © 2008 American Institute of Physics

Author complimentary copy. Redistribution subject to AIP license or copyright, see http://jap.aip.org/jap/copyright.jsp

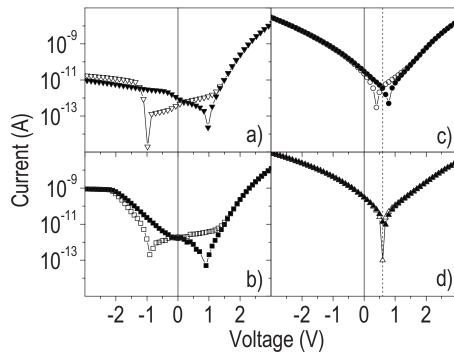

FIG. 1. *I-V* characteristics under dark (a) and under illumination with 1310 (b), 850 (c), and 633 nm (d) laser lines scanned in both directions. Closed symbols—scanning from forward to reverse direction; open symbols—scanning from reverse to forward direction. The short-dashed line is at 600 mV.

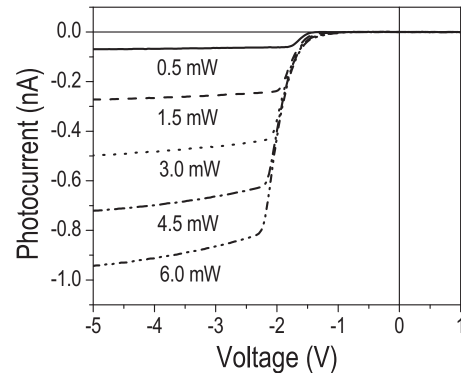

FIG. 2. Variation in photocurrent under 1310 nm excitation for different laser powers as a function of applied bias.

nanocrystal size.[25] Hence the active layer of our device is composed by a 50 nm thick silicon rich silicon oxynitride layer containing nanocrystalline silicon of average size 5 nm.

The Si-nc rich MOS structure was characterized by current-voltage (*I-V*) measurements. *I-V* characteristics were measured by an Agilent 4156C and an HP 4145A semiconductor parameter analyzer. *I-V* characteristics were recorded under dark and under illumination from the poly-Si gate side with three different focused laser wavelengths:

(1) 633 nm light to excite both Si-nc and the *p*-type doped Si substrate;
(2) 850 nm light to excite only the *p*-type doped Si substrate since it is below the band gap of Si-nc; and
(3) 1310 nm light to investigate subband gap response since this wavelength is below the band gap of both the Si-nc and Si.

In *I-V* measurements, the voltage scan was performed from both forward and reverse directions.

The spectral response under reverse bias (−5 V) in the 350–1200 nm range has been measured with a xenon arc lamp (1000 W) coupled with a double grating monochromator, while a tunable diode laser, Santech TSL-210F, has been used in the 1360–1630 nm range.

III. RESULTS AND DISCUSSIONS

I-V characteristics in dark and under illumination with three different wavelengths are shown in Fig. 1. The dark *I-V* characteristics in Fig. 1(a) are rectifying with a rectification factor of ~2000 at ±3 V. Hysteresis is observed. Current minima occur at about ±1 V during scanning from forward to reverse and reverse to forward direction, respectively, which corresponds to a hysteresis width of 2 V around 0 V.

Under illumination with 633 nm light [Fig. 1(d)] the reverse current increases by four orders of magnitude at −3 V with respect to the dark value. On the contrary, a little current increase is observed under forward bias. A small photovoltaic effect with a short circuit current of ~300 pA and an open circuit voltage of ~600 mV is evident, too. The open circuit voltage value is very similar to what usually found for microcrystalline silicon based solar cell. What is most evident in Fig. 1(d) with respect to Fig. 1(a) is a strong reduction in the hysteresis width (less than 100 mV around 600 mV).

Illumination with 850 nm light [Fig. 1(c)] also leads to a photovoltaic effect with a short circuit current of ~25 pA and an open circuit voltage of 400 mV when scanning from reverse to forward direction and of 800 mV when scanning in the opposite direction. This means that the hysteresis width in this case is 400 mV around 600 mV. The reverse current increases by three orders of magnitude at a reverse bias of −3 V with this illumination.

Illumination with 1310 nm light [Fig. 1(b)] does not lead to any photovoltaic effect but to two orders of magnitude increase in the reverse current at −3 V bias. The hysteresis width (about 1.8 V) is very close to the one found in dark conditions. The photocurrent (difference between the current with illumination and in the dark) as a function of the reverse bias under different powers of 1310 nm light is depicted in Fig. 2. The photocurrent is very small in forward bias and up to a reverse bias of ~−1 V. Below this reverse bias, the photocurrent increases first almost exponentially and then linearly.

The observed hysteresis is associated with electron or hole trapping into the SRO.[23] This causes a built-in potential that adds to the external bias. Since the built-in potential has different signs depending on the charge of the trapped particle, the hysteresis develops. The hysteresis width is associated with the density of trapped charges. The fact that this width decreases under illumination means that photocarriers either compensate the trapped charges or are generated by absorption from these trap states. The hysteresis width reduction is stronger for 633 nm than for 850 nm illumination because 850 nm light is not able to efficiently excite carriers in the Si-nc.

The spectral response of the device (responsivity) at a reverse bias of −5 V is shown in Fig. 3. Figure 3(a) shows the responsivity at short wavelengths while Fig. 3(b) depicts the same at longer wavelengths. The line shape of the responsivity in the 350–1200 nm range is very similar to that of crystalline silicon. This shows that in our device the absorption occurs mainly in the *p*-type doped Si layer since the SRO layer is very thin (50 nm). On the other hand, a weak but significant responsivity is also measured below the optical band gap of both crystalline silicon (1.1 eV) and of nano-

Author complimentary copy. Redistribution subject to AIP license or copyright, see http://jap.aip.org/jap/copyright.jsp

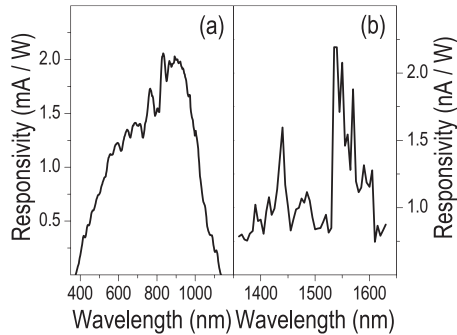

FIG. 3. Spectral response of the device (a) in 350–1200 nm range and (b) 1360–1630 nm range.

crystalline silicon in the SRO layer (1.6 eV). This absorption is not found in a control silicon solar cell, which indicates that it is due to the presence of subband gap energy levels in the SRO layer. The spectral peak at about 1550 nm in the responsivity curve can be tentatively associated to nitrogen related midband gap states formed at the Si-nc/silicon oxynitride matrix interfaces.[26] Another noticeable fact is that the photocurrent is not observed for bias lower than about −1 V (Fig. 2) when 1310 nm illumination is used. This means that the photoexcited electrons in the defect levels are not injected into the conduction band. A high reverse bias is needed to detrap these photoexcited carriers.

A simple diagram can be used to model this mechanism (Fig. 4). Here the conduction and valence bands of the layer sequence in our MOS device are simply drawn as a sequence of energy barriers (silicon oxynitride) and energy wells (Si-nc) with the addition of subband gap levels due to the interface traps for electrons at the nc-Si/silicon oxynitride interface.[27,28] The bands are tilted due to the reverse bias. Under subband gap illumination, electrons from the Si-nc valence band are photoexcited to the interface states (E_e^t) where they get trapped. If the bias is large enough, the tilting of the band is so large that tunneling of trapped electrons from the trap level (E_e^t) to the ground electron level (E_e^0) of the Si-nc is possible. This is shown in the inset of Fig. 4. In these conditions, a trap-assisted transport of electrons through the SRO is triggered, as it has been previously demonstrated to occur under forward bias without illumination.[23] A photocurrent is thus generated. With increasing reverse bias, the photocurrent increases since more and more electrons can escape by traps. Eventually, the photocurrent saturates to a value that is mostly governed by the carrier generation rate, i.e., by the illumination density. In this regime the photocurrent increases linearly with the bias as observed in Fig. 2.

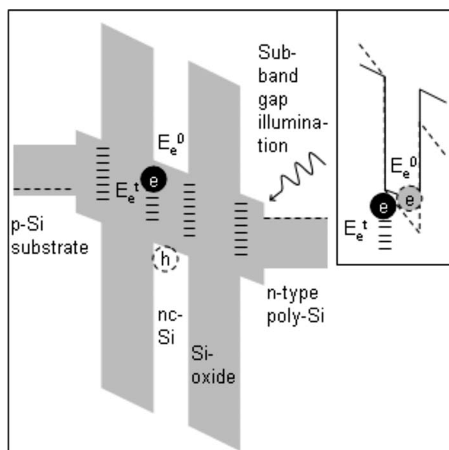

FIG. 4. Band schematic of the structure showing absorption of subband gap photons and (inset) tunneling of photogenerated carriers under reverse bias.

This model also provides a clue on the hysteresis loop formation. Under forward bias the interface states are emptied and a positive charge accumulates at the nc-Si/SiO_2 interface. Under reverse bias, the injected minority electrons are trapped at the interface states and a negative charge accumulates at the nc-Si/SiO_2 interface.

With 633 nm illumination, electrons and holes are generated both in the substrate and in the Si-nc. With a small forward bias and/or in reverse bias conditions, the electrons injected into the SRO layer recombine with the photogenerated holes. No charging thus occurs. Under forward bias, a continuous flow of electron occurs where the electrons ejected from the interface levels are replaced by photogenerated electrons. Consequently, the empty trap states are refilled. These two mechanisms both contribute to the decrease in the hysteresis width.

For 850 nm illumination, electron hole pairs are generated mainly in the *p*-type silicon. In this way only few electrons are provided to fill the shallow traps that stay mostly empty. Thus the hysteresis width is larger than for 633 nm illumination.

Under illumination with 1310 nm light, there is no chance of band to band excitation either in the substrate or in the nanocrystals. Hence, with this illumination the charging state of the SRO layer will not change, leading to very similar hysteresis as observed in dark condition.

IV. CONCLUSIONS

In this work, the photoconducting properties of MOS structure containing Si-nc embedded in silicon oxynitride matrix have been discussed. Illumination above the band gap of silicon and Si-nc with 633 nm light shows a large increase in the reverse current as well as a photovoltaic effect. On the other hand, for subband gap illumination with 1310 nm light, no photo voltaic effect is observed, while a considerable photocurrent is measured under reverse bias below a threshold voltage of ∼−1 V. A model to explain these findings points to the role of interface states in ruling the properties of SRO based MOS devices under illumination. This study reveals that these devices can be used as photodetector over a large spectral window (350–1630 nm). Furthermore, a proper design of the device may lead to significant photovoltaic effects even with illumination with light where Si is transparent. Thus, nanocrystalline silicon may be a potential material for third generation photovoltaics not only for its application in MEG solar cell[16] but also for intermediate band solar cell.

ACKNOWLEDGMENTS

The authors acknowledge the support of the research through the project "HCSC—High Concentration Solar

Author complimentary copy. Redistribution subject to AIP license or copyright, see http://jap.aip.org/jap/copyright.jsp

Cells" coordinated by OPTOI Microelectronics and the financial support by the Autonomous Province of Trento, Italy. One of the authors (S.M.H.) thanks DST, Government of India, for BOYSCAST fellowship. We thank Enrico Moser and Alessandro Marconi for laboratory assistance.

[1] S. Tiwari, F. Rana, H. Hanafi, A. Hartstein, E. F. Crabbe, and K. Chan, Appl. Phys. Lett. **68**, 1377 (1996); S. Tiwari, J. A. Wahl, H. Silva, F. Rana, and J. J. Welser, Appl. Phys. A: Mater. Sci. Process. **71**, 403 (2000).
[2] M. Porti, M. Avidano, M. Nafria, X. Aymerich, J. Carreras, O. Jambois, and B. Garrido, J. Appl. Phys. **101**, 064509 (2007).
[3] T. Z. Lu, M. Alexe, R. Scholz, V. Talalaev, R. J. Zhang, and M. Zacharias, J. Appl. Phys. **100**, 014310 (2006).
[4] S. Ossicini, L. Pavesi, and F. Priolo, *Light Emitting Silicon for Micro-Photonics*, Springer Tracts in Modern Physics Vol. 194 (Springer-Verlag, Berlin, 2003).
[5] F. Iacona, A. Irrera, G. Franzo, D. Pacifici, I. Crupi, M. Miritello, C. D. Presti, and F. Priolo, IEEE J. Sel. Top. Quantum Electron. **12**, 1596 (2006).
[6] R. J. Walters, G. I. Bourianoff, and H. A. Atwater, Nat. Mater. **4**, 143 (2005).
[7] J.-M. Shieh, Y.-F. Lai, W.-X. Ni, H.-C. Kuo, C.-Y. Fang, J. Y. Huang, and C.-L. Pan, Appl. Phys. Lett. **90**, 051105 (2007).
[8] M. A. Green, Physica E (Amsterdam) **14**, 65 (2002).
[9] M. A. Green, Prog. Photovoltaics **9**, 123 (2001).
[10] W. Shockley and H. J. Queisser, J. Appl. Phys. **32**, 510 (1961).
[11] R. T. Ross and A. J. Nozik, J. Appl. Phys. **53**, 3813 (1982).
[12] A. Marti and G. L. Araujo, Sol. Energy Mater. Sol. Cells **43**, 203 (1996).
[13] C. Strumpel, M. McCann, G. Beaucarne, V. Arkhipov, A. Slaoui, V. Svrcek, C. del Canizo, and I. Tobias, Sol. Energy Mater. Sol. Cells **91**, 238 (2007).
[14] T. Trupke, M. A. Green, and P. Wurfel, J. Appl. Phys. **92**, 1668 (2002).
[15] P. T. Landsberg, H. Nussbaumer, and G. Willeke, J. Appl. Phys. **74**, 1451 (1993).
[16] M. C. Beard, K. P. Knutsen, P. Yu, J. M. Luther, Q. Song, W. K. Metzger, R. J. Ellingson, and A. J. Nozik, Nano Lett. **7**, 2506 (2007).
[17] P. Wurfel, Sol. Energy Mater. Sol. Cells **46**, 43 (1997).
[18] D. Timmerman, I. Izeddin, P. Stallinga, I. N. Yassievich, and T. Gregorkiewicz, Nat. Photonics **2**, 105 (2008).
[19] M. Wolf, Proc. IRE **48**, 1246 (1960).
[20] T. Trupke, M. A. Green, and P. Wurfel, J. Appl. Phys. **92**, 4117 (2002).
[21] A. J. Nozik, Physica E (Amsterdam) **14**, 115 (2002).
[22] R. H. Morf, Physica E (Amsterdam) **14**, 78 (2002).
[23] S. Prezioso, A. Anopchenko, Z. Gaburro, L. Pavesi, G. Pucker, L. Vanzetti, and P. Bellutti, J. Appl. Phys. **104**, 063103 (2008).
[24] C. Delerue, G. Allan, and M. Lannoo, J. Lumin. **80**, 65 (1998).
[25] S. Takeoka, M. Fujii, and S. Hayashi, Phys. Rev. B **62**, 16820 (2000).
[26] L. E. Ramos, E. Degoli, G. Cantele, S. Ossicini, D. Ninno, J. Furthmuller, and F. Bechstedt, J. Phys.: Condens. Matter **19**, 466211 (2007).
[27] C. H. Henry, R. F. Kazarinov, H. J. Lee, K. J. Orlowsky, and L. E. Katz, Appl. Opt. **26**, 2621 (1987).
[28] K. Wörhoff, A. Driessen, P. V. Lambeck, L. T. H. Hilderink, P. W. C. Linders, and Th. J. A. Popma, Sens. Actuators, A **74**, 9 (1999).

Author complimentary copy. Redistribution subject to AIP license or copyright, see http://jap.aip.org/jap/copyright.jsp